A Near-infrared Benzothiazole-based Chemodosimeter for Rapid and Selective Detection of Hydrogen Sulfide

Safacan KOLEMEN[1,2,3]* 📧 🆔

[1]Department of Chemistry, Faculty of Science, Koc University, Sariyer, Istanbul 34450, Turkey
[2]Surface Science and Technology Center (KUYTAM), Koc University, Sariyer, Istanbul 34450, Turkey
[3]Boron and Advanced Materials Application and Research Center, Koc University, Sariyer, Istanbul 34450, Turkey

Abstract: Hydrogen sulfide (H_2S) is a biologically relevant gaseous molecule, which involves in a wide variety of physiological and pathological processes. Thus, detection of H_2S is highly valuable in order to clarify its complex roles. In this study, a new benzothiazole-based donor-acceptor type H_2S selective chemodosimeter (**HP-1**) was synthesized and its H_2S detection capabilities were investigated in aqueous solutions. **HP-1** exhibited a red-shifted absorption signal at 530 nm and a near-infrared (NIR) fluorescence peak at 680 nm as a result of enhanced intramolecular charge transfer (ICT) in the presence of H_2S, which enabled a selective and very rapid ratiometric fluorescent detection. **HP-1** was also showed to be highly sensitive toward H_2S with a very low limit of detection value.

INTRODUCTION

Hydrogen sulfide (H_2S) is an important gasotransmitter along with carbon monoxide and nitric oxide in living cells, which is endogenously produced from cysteine and cysteine derivatives in reactions that are catalyzed by cystathionine β-synthase (CBS), cystathionine γ-lyase (CSE) and 3-mercaptopyruvate sulfurtransferase (MST) (1-4). H_2S involves in fundamental signaling pathways and consequently plays crucial roles in various physiological processes such as cell growth, neurotransmission, insulin secretion, regulation of the redox balance, inflammation, angiogenesis and apoptosis (3,5). However, mismanagement of intracellular H_2S level is directly associated with the formation of serious health problems including Alzheimer's disease, Down syndrome, diabetes, hepatic cirrhosis, and cardiovascular disorders (5-8). It is also well-established that CSE and CBS enzymes are overexpressed in certain cancer cells, which makes H_2S a significant marker for cancer diagnosis (9,10). Thus, it is critical to detect and track dynamic H_2S fluxes with high selectivity and sensitivity in their native environment. Conventional detection approaches mostly rely on electrochemical analyses, gas chromatography, and metal-induced precipitation techniques, which are limited mainly due to the low sensitivity and lack of real-time imaging capability (11-13). To that end, fluorescence imaging is a highly promising tool as it offers spatial and temporal resolution, high selectivity/sensitivity, non-destructive nature, in situ detection, and cheap instrumentation (14-16). In the design of H_2S selective fluorescent agents, the most popular

approach is to employ reaction-based probes (chemodosimeters) as a result of high reactivity of H₂S. Accordingly, plenty of chemodosimeters utilizing a wide variety of reactions such as reduction of azide or nitro to amine, nucleophilic addition, thiolysis of *m*-dinitrophenyl ether and cleavage of dinitrobenzenesulfonyl moiety have been successfully reported so far in order to satisfy selective optical detection (15-19). However, majority of the reaction-based probes still suffer from the emission signals below 650 nm, which can be absorbed by biomolecules and results in autofluorescence. On the other side, near-IR (NIR) emitting probes are quite attractive as the NIR signal does not interfere with the biological fluorophores as well as allows deeper tissue penetration (20). Thus, a great deal of effort has been put to develop H₂S-selective NIR chemodosimeters, (15,20-23), however there are still some challenges need to be addressed in order to improve the impact of NIR probes such as slow response rates, low fluorescence quantum yields and small Stokes shifts.

Donor-π-acceptor (D-π-A) dyes have attracted great interest as fluorescent probes in recent years since they possess strong NIR emission signals and large Stokes' shifts in aqueous solutions, and they can be easily obtained through a well-established chemistry (24-27). In a typical design approach, a phenol group, which acts as a donor, is attached to acceptor moieties, which results in a π-conjugated system. Deprotonation of the phenol in physiological conditions or removing the cage group on the phenol with an analyte of interest yields a phenolate that initiates intramolecular charge transfer (ICT) process by triggering the donation of π-electrons from phenolate to conjugated acceptor units (24). This causes a remarkable red-shift in the absorption signal of the probe and generates a strong NIR emission, which allows both ratiometric and OFF-ON type detection (24). Benzothiazole is among the promising acceptor units, which have been used successfully in the design of D-π-A type chemodosimeters for imaging of several analytes (23,28,29). In this study, a H₂S selective benzothiazole-based chemodosimeter (**HP-1**) (Figure 1) was developed as a (D-π-A) type probe and its H₂S detection capabilities were evaluated in detail by UV-Vis and fluorescence spectroscopies in aqueous solutions.
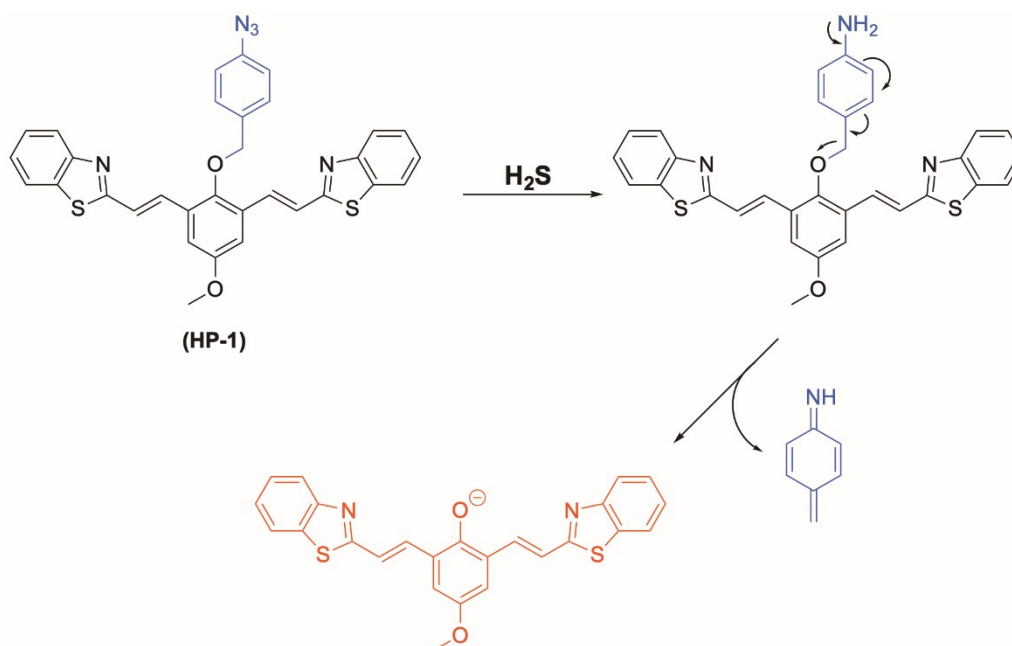

Figure 1. Structure of **HP-1** and its activation mechanism in the presence of H₂S.

EXPERIMENTAL

Chemicals and Apparatus
Reagents were purchased from Sigma-Aldrich or Merck and used without further purification. All dry solvents used in reactions were directly obtained from the Mbraun MBSPS5 solvent drying system. Sodium sulfide nonahydrate Na₂S·9H₂O was purchased from Sigma-Aldrich and stored at 2-8 °C. Deuterated solvents were purchased from Eurisotop and used as received. Column chromatography was performed by using thick-walled glass columns and silica gel (Merck 230-400 mesh). Thin layer chromatography (TLC Merck Silica Gel 60 F254) was performed by using commercially prepared 0.25 mm silica gel plates

and visualization was provided by UV lamp. The relative proportions of solvents in chromatography solvent mixtures refer to the volume: volume ratio.

Instruments
^1H and ^{13}C NMR spectra were recorded on a Bruker Avance III Ultrashield 500 MHz NMR spectrometer using $CDCl_3$ or d_6-DMSO as the solvents. Chemical shifts are reported in ppm. Coupling constants (J) are reported in hertz (Hz), and the spin multiplicities were specified by the following symbols: s (singlet), d (doublet), t (triplet), and m (multiplet). NMR spectra were processed with MestReNova software. UV−Visible spectra were acquired on a Shimadzu UV-3600 UV-Vis-NIR spectrophotometer. Fluorescence spectra were collected on an Agilent Cary Eclipse spectrophotometer. Fluorescence quantum yield of the samples were investigated by using a fluorescence spectrometer (FLS 1000, Edinburgh Instruments) with an integrating sphere accessory. Mass spectra were recorded on Waters Synapt G1 High-Definition mass spectrometer.

Synthesis
1-azido-4-(bromomethyl)benzene **(2)** (30) and compound **(4)** (23) were synthesized according to literature reports (Figure 2).

Synthesis of HP-1
Compound **4** (50 mg, 0.12 mmol) was dissolved in dry ACN (10 mL) and K_2CO_3 (636 mg, 4.6 mmol) was added to the resulting solution. The solution was stirred at room temperature for 15 minutes and compound **2** (31 mg, 0.15 mmol) was added to the reaction mixture. The reaction was stirred overnight at room temperature. The crude mixture was diluted with DCM (100 mL) and washed with brine (100 mL). Organic layer was separated and dried over Na_2SO_4. The crude product was purified by column chromatography on silica gel (*n*-hexane/EtOAc, 2/1) to give yellow-white solid (58% yield, 38 mg). ^1H NMR (500 MHz, $CDCl_3$, ppm) δ 8.02 (d, J = 8.1 Hz, 2H), 7.89 (d, J = 8.0 Hz, 2H), 7.74 (d, J = 16.3 Hz, 2H), 7.51 – 7.39 (m, 8H), 7.20 (s, 2H), 7.03 (d, J = 8.1 Hz, 2H), 4.87 (s, 2H), 3.89 (s, 3H). ^{13}C NMR (126 MHz, $CDCl_3$, ppm) δ 166.9, 156.3, 153.9, 149.6, 140.5, 134.3, 132.7, 132.1, 130.9, 130.7, 126.4, 125.7, 124.2, 123.1, 121.6, 119.4, 112.8, 77.7, 55.7. HRMS m/z calc. for $C_{32}H_{23}N_5O_2S_2$: 574.1293 [M+H]$^+$; found: 574.1371.

Photophysical measurements
Stock solution of **HP-1** was prepared in DMF and then diluted with PBS (pH 7.4) to final concentrations before each measurement. $Na_2S \cdot 9H_2O$ stock solution was prepared in PBS (pH 7.4). 3 mL quartz cells were used, and the slit

widths were set up as 10 nm for both emission and excitation.

Fluorescence quantum yield calculation
Fluorescence quantum yield of the sample was investigated by using a fluorescence spectrometer with an integrating sphere accessory. A continuous-wave xenon lamp was used as the excitation source and the emitted fluorescence was detected with a standard photomultiplier (PMT-900) covering a wavelength range of 200-900 nm. During the measurements, the PMT was cooled down to -20 °C by using a built-in housing to reduce the undesired dark current noise.

For quantum yield measurement, an integrating sphere was placed inside the sample compartment of the spectrometer. Internal cavity of the sphere was coated with a PTFE-like material to enable a reflectance of approximately >95% over the wavelength range between 400 and 1500 nm (250 and 2500 nm). Prior to the experiments performed with the sample, the blank spectrum was measured by using the reference solvents (PBS (pH 7.4, 50% DMF)). In order to cover a scattering range, the emission scans were started from 20 nm below the actual excitation wavelength (510 nm) and finished at 900 nm. Furthermore, the step size and the integration time of the measurements were set to 1 nm and 0.2 seconds, respectively. After all the emission measurements of the samples and references were complete, the quantum yield of the sample was determined by using the Fluoracle® software. The built-in analysis tool calculated the quantum yield (QY) by following Eq. (1).

$$QY = \frac{E_s - E_B}{S_B - S_s} \qquad (1)$$

where E_s (E_B) and S_s (S_B) are the selected areas for the emitted and scattered signals of the sample (blank).

Limit of detection (LOD) calculation
The limit of detection was calculated according to formula given below, where m is the slope of the emission intensity at 680 nm versus Na_2S concentration graph and s is the standard deviation of the 6 blank measurements. LOD was calculated according to Eq. (2).

$$LOD = 3s/m \qquad (2)$$

RESULTS AND DISCUSSION

In the design of **HP-1**, two benzothiazole acceptor units were conjugated to donor *p*-methoxyphenol core and a H_2S-cleavable azido group was used as a cage moiety to mask the phenol. Removal of the cage group upon H_2S-induced selective reduction of azide to amine causes a red-shift in both absorption and emission signals of **HP-1**, which reveals a ratiometric fluorescence sensor for detection of H_2S (Figure 1). Synthesis of **HP-1** was depicted in Figure 2. Initially, 4-aminobenzyl alcohol was treated with NaN_3 in the presence of

$NaNO_2$ to get 4-azidobenzylalcohol **(1)**. Then **(1)** was reacted with PBr_3 and the cage unit 4-azidobenzyl bromide **(2)** was obtained. For the probe core synthesis, commercially available 4-methoxyphenol was formylated by running a Duff reaction to give 2,6-diformyl-4-methoxyphenol **(3)**, which was then converted to **(4)** via Knoevenagel condensation. Finally, the cage unit **(2)** was attached to **(4)** in dry acetonitrile and **HP-1** was attained in a moderate yield. **HP-1** was characterized by ^1H NMR, ^{13}C NMR and high-resolution mass spectrometry (HR-MS) (Figure S1-S3).
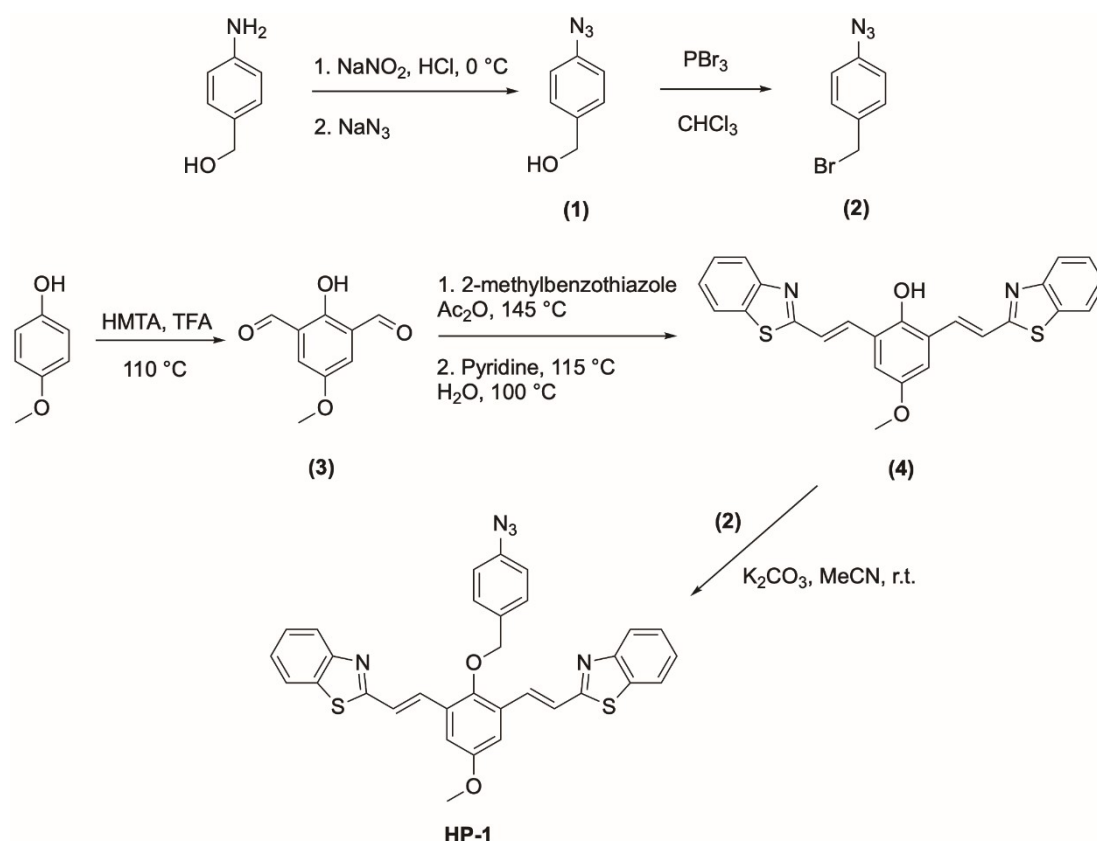

Figure 2. Synthetic pathway for **HP-1**.

After completing the synthesis, the optical responses of **HP-1** to H_2S were investigated with UV-Vis and fluorescence spectrophotometers in aqueous PBS solution (pH 7.4, 50% DMF) (Figures 3 and 4). In all the experiments, H_2S was generated *in situ* by adding Na_2S into a PBS buffered solution (pH 7.4) as in the case of literature examples (15). The pKa of H_2S is 7, thus the Na_2S solution in PBS at pH 7.4 contains HS^- and S^{2-} anions in addition to H_2S, which, in fact, mimics the speciation in the cellular environment (15). **HP-1** exhibited strong but short wavelength absorption peak centered at 335 nm (ε = 23100 $M^{-1}cm^{-1}$) as a result of blocked electron donation from donor core to acceptor units (Figure 3a). Upon

treating **HP-1** (20 µM) with Na_2S (200 µM), absorption peak at 335 nm was slightly decreased and a concomitant red-shifted peak appeared at 530 nm (ε = 6600 $M^{-1}cm^{-1}$) with an isosbestic point at 420 nm, which can be also detected by naked eye as colorless **HP-1** solution turned to pale pink after the addition of Na_2S. This result indicates that **HP-1** reacts readily with H_2S and uncages the phenol, which switches on the ICT process. A gradual increase in the absorption signal at 530 nm was also determined when **HP-1** was titrated with increasing concentrations of Na_2S (0-200 µM) (Figure 3b, Figure S5a).

In the case of fluorescence measurements, a characteristic NIR emission signal at 680 nm appeared gradually as the Na_2S concentration (0-200 μM) increased (up to 130-fold, φ_F = 11%) upon excitation at newly formed absorption peak at 530 nm (Figure 4 a,b, Figure S5b). When the excitation wavelength was adjusted to 420 nm (isosbestic point), emission peak of the parent **HP-1** at 470 nm was decreased and broad NIR fluorescence signal was observed between 650-750 nm with a maximum at 680 nm (Figure 4c), suggesting that **HP-1** can act as a NIR ratiometric probe. Both changes in absorption and emission signals were accomplished in seconds, clearly indicating that **HP-1** works much faster than most of the current H_2S selective probes and can rapidly detect H_2S. It is also important to note that **HP-1** exhibited a large Stokes' shift ($\sim$150 nm) (Figure 4d), which is another critical parameter for a fluorescent probe.
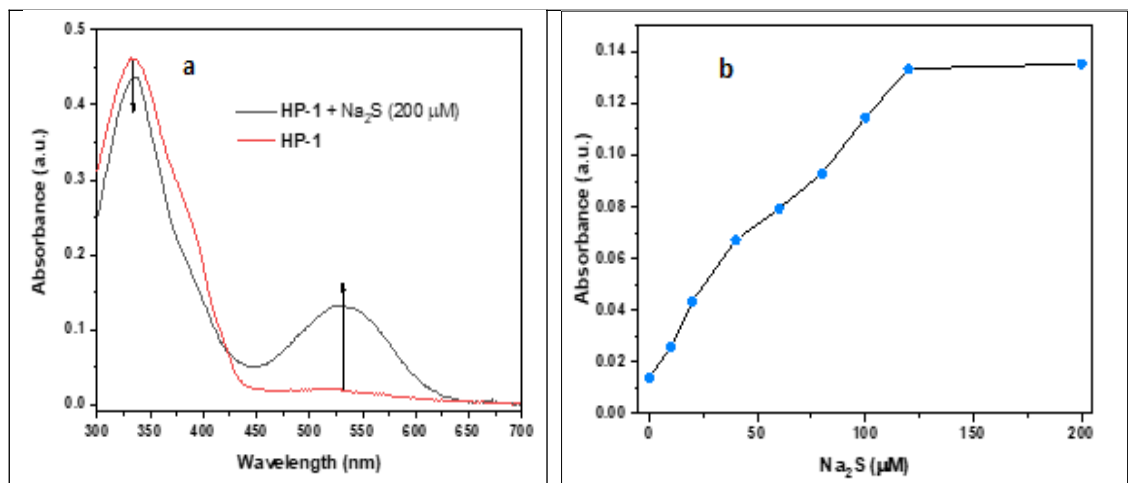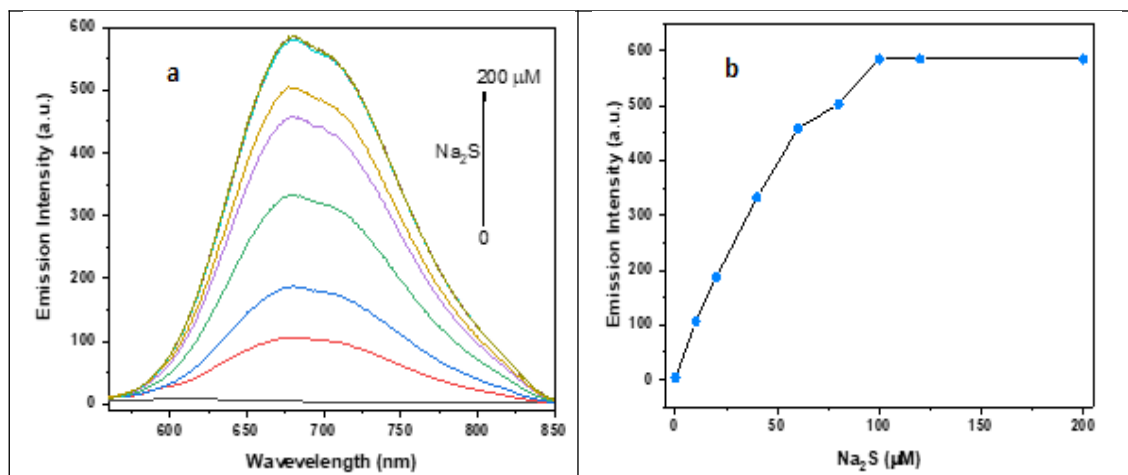
Figure 3. (a) Absorption spectra of **HP-1** (20 μM) before and after addition of Na_2S (200 μM) and (b) absorption signal of **HP-1** (20 μM) at 530 nm in increasing Na_2S concentrations in PBS (pH 7.4, 50% DMF).
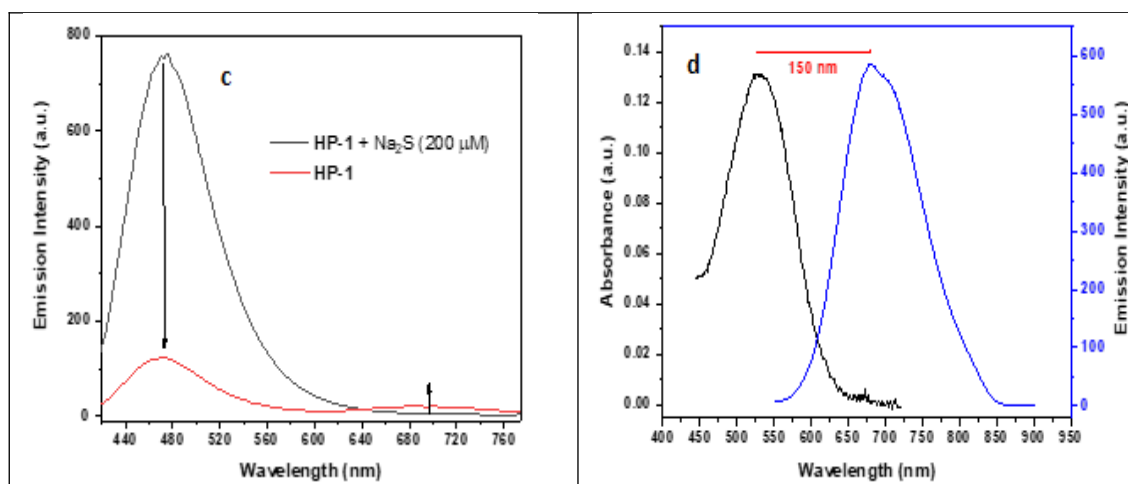
Figure 4. (a) Emission spectra of **HP-1** (20 μM) upon addition of increasing Na$_2$S concentrations and (b) the relationship between the emission intensities of **HP-1** (20 μM) at 680 nm and the concentration of Na$_2$S. Excitation wavelength is 530 nm. (c) Emission spectra of **HP-1** (20 μM) before and after addition of Na$_2$S (200 μM). Excitation wavelength is 420 nm. (d) The Stokes' shift of **HP-1** (20 μM) after addition of Na$_2$S (200 μM). Excitation wavelength is 530 nm. All experiments were done in PBS (pH 7.4, 50% DMF).

Next, the selectivity of **HP-1** towards H$_2$S was checked by using biologically relevant nucleophilic species including bio-thiols such as glutathione (GSH), cysteine (Cys) and homocysteine (Hcy) as well as different metal ions. No detectable change was observed both in absorption and emission spectra (Figure 5), proving the high selectivity of

HP-1 for H$_2$S over other species. The sensitivity of **HP-1** was measured by calculating the limit of detection (LOD) value and found to be as low as 0.64 μM. Finally, H$_2$S-induced removal of the cage group and the release of compound **4** was confirmed by acquiring a high-resolution mass spectrum (Figure S4).
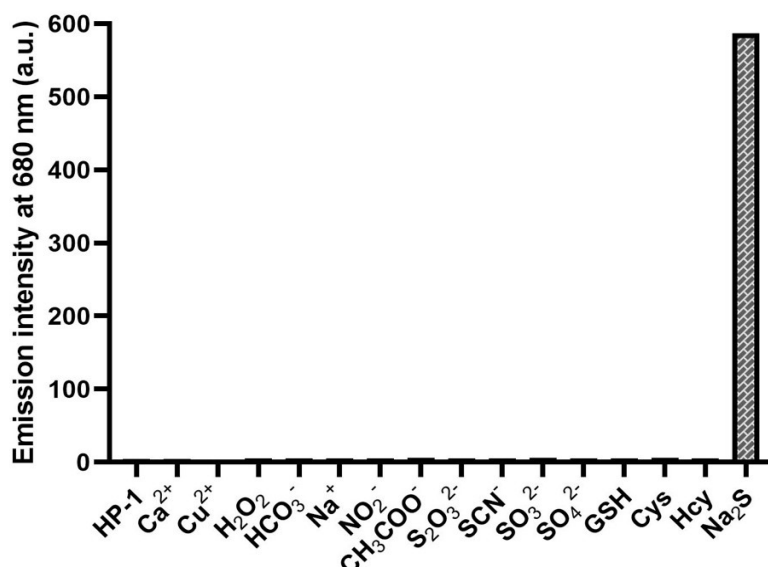

Figure 5. Emission intensities of **HP-1** (20 μM) in the absence and presence of different analytes in PBS (pH 7.4, 50% DMF). Na$_2$S concentration was 200 μM. All other analyte concentrations were set to 1 mM.

CONCLUSION

In summary, an easily accessible H$_2$S-selective benzothiazole-based chemodosimeter (**HP-1**) was

synthesized and its molecular structure as well as optical responses to H$_2$S were characterized. Upon addition of Na$_2$S, **HP-1** exhibited a 195 nm bathochromic shift in the absorption signal and a

noticeable concentration dependent increase in the NIR emission at 680 nm as a result of enhanced ICT process, which was triggered by the removal of the azido cage group. Remarkably, all of these changes in photophysical parameters were realized in seconds with high sensitivity and selectivity towards H_2S.

CONFLICT OF INTEREST

The author declares no conflict of interest.

ACKNOWLEDGEMENTS

REFERENCES

1. Qian Y, Karpus J, Kabil O, Zhang S-Y, Zhu H-L, Banerjee R, et al. Selective fluorescent probes for live-cell monitoring of sulphide. Nat Commun. 2011 Sep;2(1):495.

2. Olas B. Hydrogen sulfide in signaling pathways. Clinica Chimica Acta. 2015 Jan;439:212–8.

3. Rose P, Moore PK, Zhu YZ. H2S biosynthesis and catabolism: new insights from molecular studies. Cell Mol Life Sci. 2017 Apr;74(8):1391–412.

4. Wang R. The Gasotransmitter Role of Hydrogen Sulfide. Antioxidants & Redox Signaling. 2003 Aug;5(4):493–501.

5. Papapetropoulos A, Pyriochou A, Altaany Z, Yang G, Marazioti A, Zhou Z, et al. Hydrogen sulfide is an endogenous stimulator of angiogenesis. Proceedings of the National Academy of Sciences. 2009 Dec 22;106(51):21972–7.

6. Wei H-J, Li X, Tang X-Q. Therapeutic benefits of H2S in Alzheimer's disease. Journal of Clinical Neuroscience. 2014 Oct 1;21(10):1665–9.

7. Szabó C. Hydrogen sulphide and its therapeutic potential. Nature Reviews Drug Discovery. 2007 Nov 1;6(11):917–35.

8. Kamoun P, Belardinelli M-C, Chabli A, Lallouchi K, Chadefaux-Vekemans B. Endogenous hydrogen sulfide overproduction in Down syndrome. American journal of medical genetics. 2003;116(3):310–1.

9. Wang L, Cai H, Hu Y, Liu F, Huang S, Zhou Y, et al. A pharmacological probe identifies cystathionine β-synthase as a new negative regulator for ferroptosis. Cell Death Dis. 2018 Oct;9(10):1005.

10. Breza J, Soltysova A, Hudecova S, Penesova A, Szadvari I, Babula P, et al. Endogenous H2S producing enzymes are involved in apoptosis induction in clear cell renal cell carcinoma. BMC Cancer. 2018 May 24;18(1):591.

11. Lawrence NS, Davis J, Jiang L, Jones TGJ, Davies SN, Compton RG. The Electrochemical Analog of the Methylene Blue Reaction: A Novel Amperometric Approach to the Detection of Hydrogen Sulfide. Electroanal. 2000;12(18):1453–60.

12. Choi MG, Cha S, Lee H, Jeon HL, Chang S-K. Sulfide-selective chemosignaling by a Cu2+ complex of dipicolylamine appended fluorescein. Chem Commun. 2009;(47):7390.

13. Furne J, Saeed A, Levitt MD. Whole tissue hydrogen sulfide concentrations are orders of magnitude lower than presently accepted values. American Journal of Physiology-Regulatory, Integrative and Comparative Physiology. 2008 Nov;295(5):R1479–85.

14. Qian Y, Zhang L, Ding S, Deng X, He C, Zheng XE, et al. A fluorescent probe for rapid detection of hydrogen sulfide in blood plasma and brain tissues in mice. Chem Sci. 2012;3(10):2920.

15. Lin VS, Chen W, Xian M, Chang CJ. Chemical probes for molecular imaging and detection of hydrogen sulfide and reactive sulfur species in biological systems. Chem Soc Rev. 2015;44:4596–618.

16. Liu C, Pan J, Li S, Zhao Y, Wu LY, Berkman CE, et al. Capture and Visualization of Hydrogen Sulfide by a Fluorescent Probe. Angew Chem. 2011 Oct 24;123(44):10511–3.

17. Lippert AR, New EJ, Chang CJ. Reaction-Based Fluorescent Probes for Selective Imaging of Hydrogen Sulfide in Living Cells. J Am Chem Soc. 2011 Jul 6;133(26):10078–80.

18. Liu Y, Feng G. A visible light excitable colorimetric and fluorescent ESIPT probe for rapid and selective detection of hydrogen sulfide. Org Biomol Chem. 2014;12:438–45.

19. Guo Z, Park S, Yoon J, Shin I. Recent progress in the development of near-infrared fluorescent probes for bioimaging applications. Chem Soc Rev. 2014;43(1):16–29.

20. Gong S, Zhou E, Hong J, Feng G. Nitrobenzoxadiazole Ether-Based Near-Infrared Fluorescent Probe with Unexpected High Selectivity for H 2 S Imaging in Living Cells and Mice. Anal Chem. 2019 Oct 15;91(20):13136–42.

21. Ozdemir T, Sozmen F, Mamur S, Tekinay T, Akkaya EU. Fast responding and selective near-IR Bodipy dye for hydrogen sulfide sensing. Chem Commun. 2014;50:5455–7.

22. Zheng Y, Zhao M, Qiao Q, Liu H, Lang H, Xu Z. A near-infrared fluorescent probe for hydrogen sulfide in living cells. Dyes and Pigments. 2013 Sep 1;98(3):367–71.

23. Zhang X, Zhang L, Ma W-W, Zhou Y, Lu Z-N, Xu S. A Near-Infrared Ratiometric Fluorescent Probe for Highly Selective Recognition and Bioimaging of Cysteine. Frontiers in Chemistry. 2019;7:32.

24. Karton-Lifshin N, Albertazzi L, Bendikov M, Baran PS, Shabat D. "Donor–Two-Acceptor" Dye Design: A Distinct Gateway to NIR Fluorescence. J Am Chem Soc. 2012 Dec 19;134(50):20412–20.

25. Chen C, Fang C. Devising Efficient Red-Shifting Strategies for Bioimaging: A Generalizable Donor-Acceptor Fluorophore Prototype. Chem Asian J. 2020;15:1514–23.

26. Jaswal S, Kumar J. Review on fluorescent donor–acceptor conjugated system as molecular probes. Materials Today: Proceedings. 2020;26:566–80.

27. Woo S-J, Kim Y, Kim M-J, Baek JY, Kwon S-K, Kim Y-H, et al. Strategies for the Molecular Design of Donor–Acceptor-type Fluorescent Emitters for Efficient Deep Blue Organic Light Emitting Diodes. Chem Mater. 2018 ubat;30(3):857–63.

28. Gong Y, Feng D, Liu W, Fang J, Feng S. A self-immolative near-infrared probe based on hemi-benzothiazolecyanine for visualizing hydrogen peroxide in living cells and mice. Dyes and Pigments. 2021 Feb;186:108954.

29. Zhang X, Liu J-Y. Solvent dependent photophysical properties and near-infrared solid-state excited state intramolecular proton transfer (ESIPT) fluorescence of 2,4,6-trisbenzothiazolylphenol. Dyes and Pigments. 2016 ubat;125:80–8.

30. Li S-J, Li Y-F, Liu H-W, Zhou D-Y, Jiang W-L, Ou-Yang J, et al. A Dual-Response Fluorescent Probe for the Detection of Viscosity and H 2 S and Its Application in Studying Their Cross-Talk Influence in Mitochondria. Anal Chem. 2018 Aug 7;90(15):9418–25.

A Near-infrared Benzothiazole-based Chemodosimeter for Rapid and Selective Detection of Hydrogen Sulfide

Safacan KOLEMEN[1,2,3]*

[1]Department of Chemistry, Faculty of Science, Koc University, Sariyer, Istanbul 34450, Turkey
[2]Surface Science and Technology Center (KUYTAM), Koc University, Sariyer, Istanbul 34450, Turkey
[3]Boron and Advanced Materials Application and Research Center, Koc University, Sariyer, Istanbul 34450, Turkey
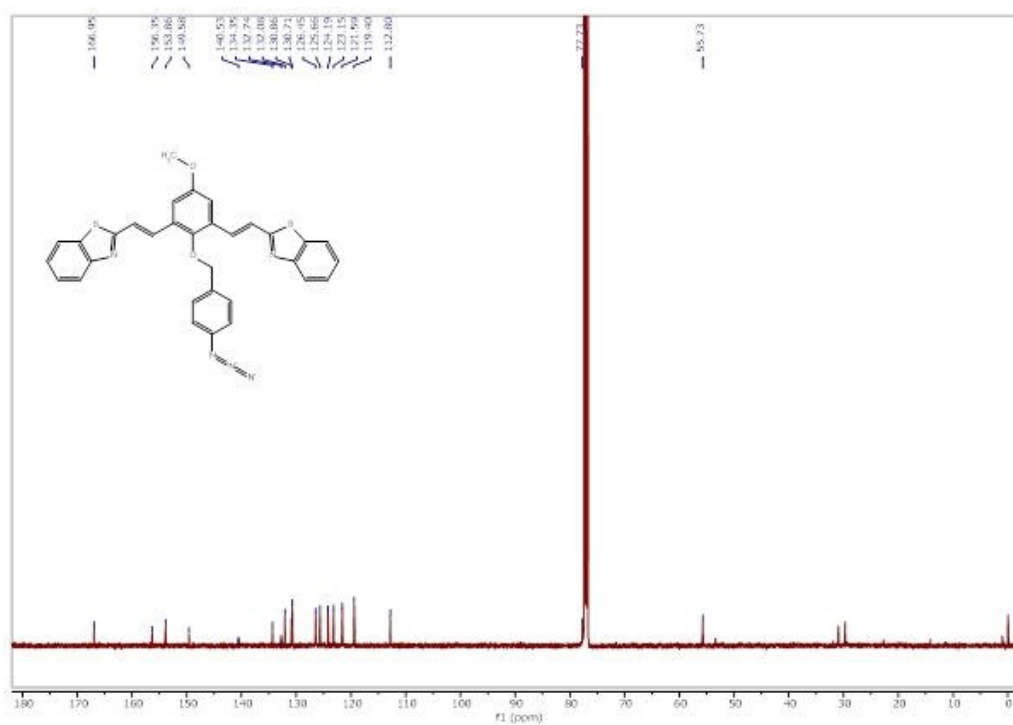
NMR Spectra
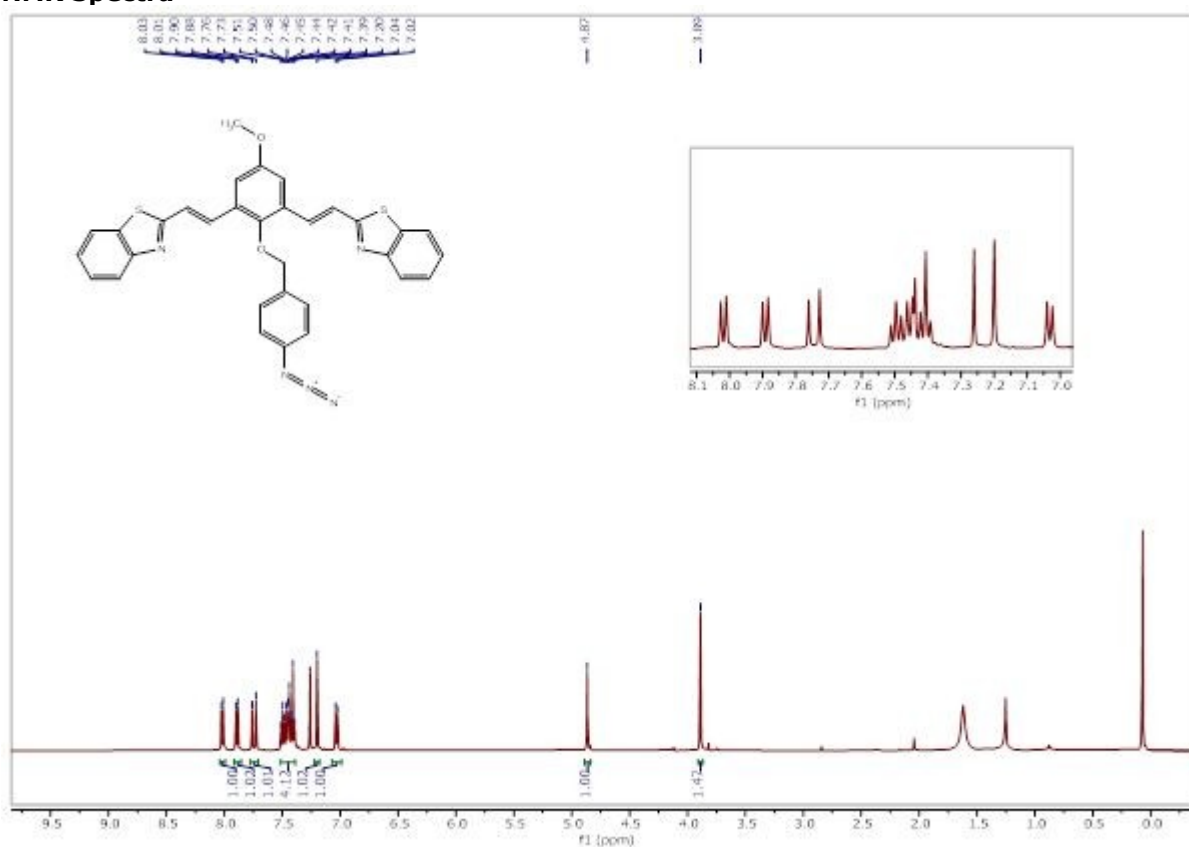
Figure S1. ^{1}H NMR spectrum of **HP-1**.
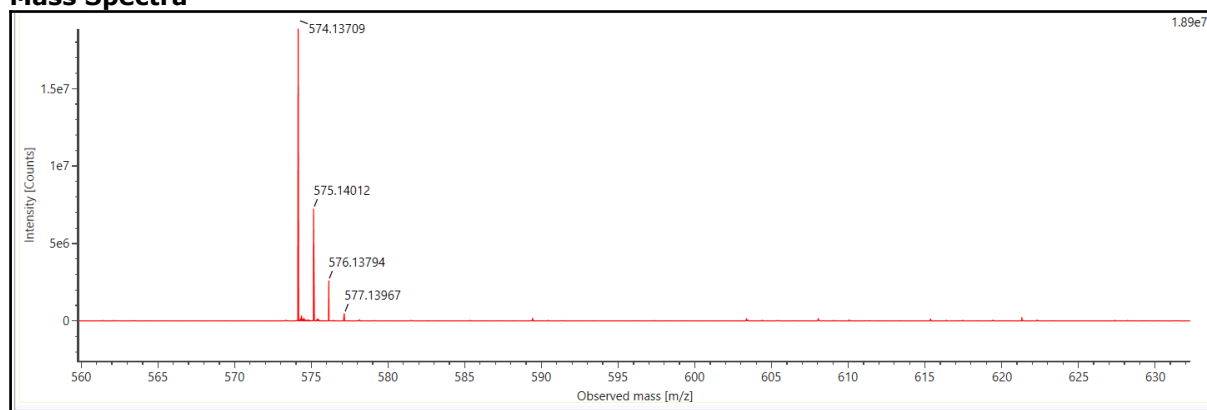
Figure S2. ^{13}C NMR spectrum of HP-1.

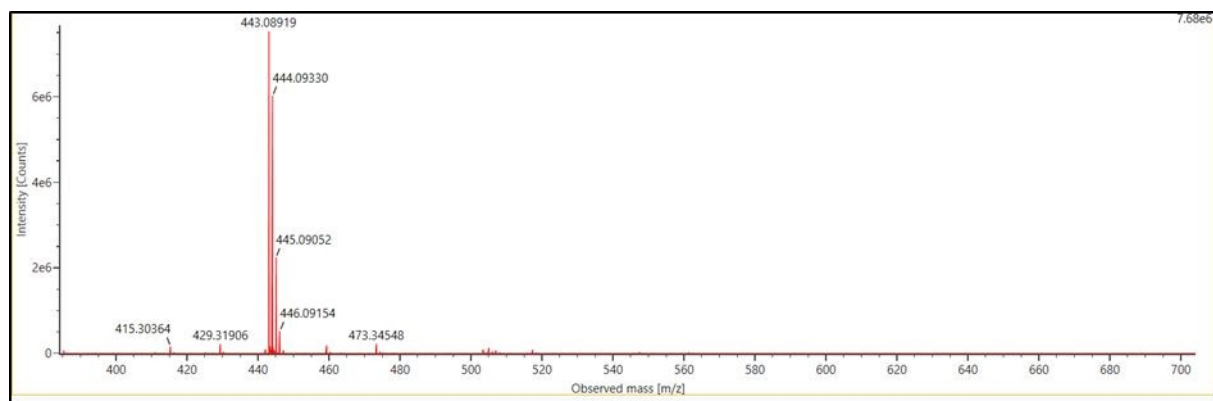**Mass Spectra**

Figure S3. HR-MS spectrum of **HP-1**.

Figure S4. HR-MS spectrum of **HP-1** + Na$_2$S. Calc. for C$_{25}$H$_{18}$N$_2$O$_2$S$_2$ 443.0810 [M+H]$^+$; found: 443.0892.
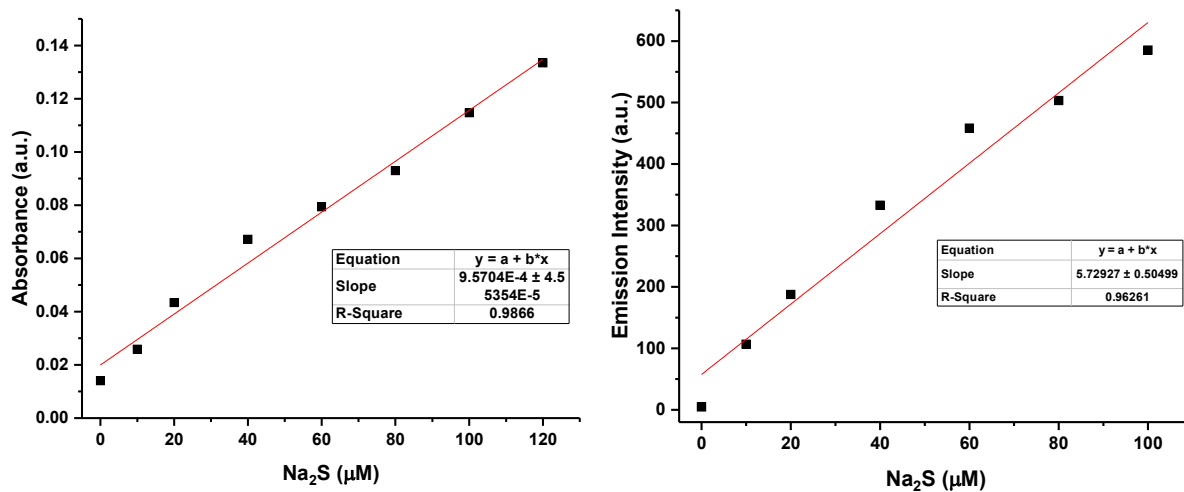
Photophysical characterization

Figure S5. Increase of the absorption signal (left) of **HP-1** (20 μM) at 530 nm and emission signal (right) at 680 nm in increasing Na$_2$S concentrations in PBS (pH 7.4, 50% DMF) in the linear concentration range.